Available online at www.sciencedirect.com

SCIENCE DIRECT®

Gynecologic Oncology 99 (2005) S16 – S23

Gynecologic Oncology

www.elsevier.com/locate/ygyno

Original Research Report

Subvisual chromatin changes in cervical epithelium measured by texture image analysis and correlated with HPV

Martial Guillaud[a], Karen Adler-Storthz[b], Anais Malpica[c], Gregg Staerkel[c], Jasenka Matisic[d], Dirk Van Niekirk[d], Dennis Cox[e], Neal Poulin[a], Michele Follen[f,g,*], Calum MacAulay[a]

[a]*Department of Cancer Imaging, BC Cancer Agency, Vancouver, British Columbia, Canada*
[b]*Department of Diagnostic Sciences, The University of Texas Health Science Center at Houston-Dental Branch, Houston, TX, USA*
[c]*Department of Pathology, The University of Texas M. D. Anderson Cancer Center, Houston, TX, USA*
[d]*Department of Pathology, BC Cancer Agency, Vancouver, British Columbia, Canada*
[e]*Department of Statistics, Rice University, Houston, TX, USA*
[f]*Department of Gynecologic Oncology, Center for Biomedical Engineering, The University of Texas M. D. Anderson Cancer Center, Houston, TX, USA*
[g]*Department of Obstetrics, Gynecology and Reproductive Sciences, The University of Texas Health Science Center at Houston, Houston, TX, USA*

Available online 26 September 2005

Abstract

Objectives. In this study, we are testing the hypothesis that human papillomavirus (HPV) positivity is correlated with chromatin texture in the cell. Interim analyses are important since this study involves 2000 patients and generates 6000 biopsy specimens that will be subjected to quantitative histopathological analysis and correlated to HPV positivity as measured by the Hybrid Capture II test (Digene; Gaithersberg, MD) and both HPV–DNA and mRNA by the polymerase chain reaction (PCR). The studies of optical technologies, from which we derive this sample, use the colposcopically directed and histopathologically classified cervical biopsy as the gold standard. In this report, we describe the results of an interim analysis of quantitative histopathology and chromatin texture as correlates of HPV infection using the cytosavant system in cytologically and histopathologically negative specimens.

Methods. A group of 1544 patients entered the optical technology trials, generating 3275 biopsies and 1544 Papanicolaou readings. Two hundred forty-eight patients were cytologically and histopathologically negative. Study pathologists reviewed histologic samples 3 times in a blinded fashion. Non-overlapping, quantitatively stained nuclei were selected from the samples by the pathologists. HPV testing was done using the PCR method and the Hybrid Capture II test. Statistical analysis involved the creation of a classification matrix using a linear discriminant analysis. The matrix was trained on HPV-positive cells by PCR. The analysis included the random creation of both a training set and a validation set that were classified based on the discrimination score obtained by correlating nuclear texture with HPV positivity.

Results. The sensitivity of the classification was 52–54% and the specificity was 77–78%. Overall, a 68% predicted accuracy was achieved for both the training set and the test set. The agreement of a test and training set shows that the sets created randomly are indeed similar, and that the discrimination score worked equally well in both sets of cells. Once a cell-by-cell algorithm for HPV positivity was derived, HPV positivity was recalculated on the basis of cell-by-cell texture features. HPV positivity was then recalculated on both a per-biopsy basis and a per-patient basis. For HPV 16 and 18, the positivity rate was 70% on a per-biopsy basis and 73% on a per-patient basis.

Conclusions. Although these results are preliminary, they suggest that texture features reflecting chromatin condensation may correlate with HPV positivity. The current sample is histologic, the analysis suggests that in a cytologic sample, HPV positivity could be detected or confirmed by texture features computed as part of an HPV-associated score. Additional biologic markers could be used as needed. While this study was performed on histologic samples, a study of cytologic samples would be more useful. Future studies will examine chromatin texture compared to HPV integration and mRNA HPV expression.

Keywords: Human papillomavirus; HPV–DNA test; Quantitative histopathology; Stoichiometric staining; Chromatin texture; Quantitative image analysis

* Corresponding author. Department of Gynecologic Oncology, Center for Biomedical Engineering, The University of Texas M. D. Anderson Cancer Center, Unit 193, 1515 Holcombe Blvd., Houston, TX 77030, USA. Fax: +1 713 792 4856.
E-mail address: mfollen@mdanderson.org (M. Follen).

0090-8258/$ - see front matter © 2005 Elsevier Inc. All rights reserved.
doi:10.1016/j.ygyno.2005.07.037

Introduction

Although the molecular mechanisms of human papillomavirus (HPV)-induced carcinogenesis are well understood, it was not until sensitive molecular testing became available that epidemiologists could verify HPV's causal role in cervical cancer [1]. The currently accepted care guidelines in the United States now include testing for this important risk factor in women older than 35 years [2]. However, this currently involves using a separate test, the Hybrid Capture II assay (Digene Corporation, Gaithersburg, MD), which adds to the cost of evaluation and or treatment.

Many investigators have suggested that the principal advantage of the liquid preparations of the Papanicolaou (Pap) smear is that they also allow reflex testing for HPV to be performed using the Hybrid Capture II assay (Digene Corporation, Gaithersburg, MD [3]). However, it would be even less expensive if the same quantitative reading of the Pap smear used to yield a clinical diagnosis could also be used to yield an HPV diagnosis using a less expensive test than the Hybrid Capture II assay [4–6].

As part of an interim analysis, we are exploring what quantitative changes can be detected in specimens from cytologically negative and histopathologically negative patient samples that are HPV positive and negative by polymerase chain reaction (PCR) [7]. We hypothesize that texture features in the histologic specimen might predict which tissue specimens are HPV positive by PCR, despite their clinically negative cytology and pathology samples [8–12].

Materials and methods

Materials

The study was conducted at The University of Texas M. D. Anderson Cancer Center (Houston, TX) and the British Columbia (BC) Cancer Agency at the University of British Columbia (Vancouver, BC). Women aged 18 and older were enrolled in the study, and informed consent was obtained from each participant. The protocols were approved by the internal review boards at the University of Texas M. D. Anderson Cancer Center, the University of Texas at Austin, and the BC Cancer Agency.

The study consists of two components: a screening study and a diagnostic study. In the screening study, patients are recruited with a history of normal Pap smears; and in the diagnostic study, patients are recruited with abnormal Pap smears. All patients undergo complete history and physical exam and HPV testing. Pan-colposcopy (colposcopy of the vulva, vagina, and cervix) was performed. Each patient underwent colposcopy of the cervix and the colposcopically directed normal and abnormal sites were identified, measured with fluorescence and reflectance spectroscopy, and then biopsied. The biopsy specimens were fixed in buffered formalin and embedded in paraffin blocks. Specimens from each patient were collected for both Hybrid Capture II and for quantitative PCR analysis of the DNA and RNA of HPV 16, HPV 18, and other high-risk types of HPV.

Three adjacent sections are cut into 4-μm sections and stained with hematoxylin and eosin (H&E). These sections are used for conventional cytologic and histopathologic clinical readings. The adjacent sections are stained with the thionine–Feulgen stain. This staining has been shown to be stoichiometric in that the intensity of the staining is related to the DNA content. More importantly for this study, nuclear texture features can be quantified giving a reproducible measure of the stippling of chromatin.

Pathology review

The first pathology review is done by one of the gynecologic pathologists on clinical duty at each institution. A second blinded review is performed by one of our study pathologists. In cases of discrepancies between the two readings, the slide is read a third time by the study pathologist to arrive at the final consensus diagnosis.

During the second review, the pathologist stores a digital picture of the diagnostic area in the study database. As part of the National Cancer Institute Program Project, 10% of the slides from M. D. Anderson are read at the BC Cancer Agency, and 10% of the slides from the BC Cancer Agency are read at M. D. Anderson. Additionally, an experienced gynecologic pathologist outside both institutions is reviewing 10% of all the slides. For any slides for which there is a two-grade difference between readings one and two (e.g., cervical intraepithelial neoplasia CIN 1 to CIN 3, LGSIL to HGSIL, satisfactory for reading versus unsatisfactory), the slides are reviewed a fourth and fifth time at M. D. Anderson and the BC Cancer Agency to reach a consensus diagnosis, and a sixth time by our consulting pathologist. A manuscript describing the clinical agreement is in submission. Overall, at interim analysis there has been 76% exact agreement in the clinical readings among pathologists at the two sites, with a kappa score of 0.736 indicating very good agreement (data not shown).

Samples

The histologic samples selected for this analysis were read in blinded fashion, as described. Those selected were from patients who had normal Pap smear and histopathologic biopsies. Each sample was mapped for image analysis. The basal layer is adjacent to the basement membrane, and the cells that make up this layer are characterized by the presence of oval nuclei. The parabasal layer is adjacent to the basal layer and also consists of cells with oval nuclei. The intermediate layer has cells with polyhedral nuclei and more cytoplasm than the cells of the other layers. Cells closer to the surface are also rounder and smaller than those in the deeper layers. Cells in the superficial layer have small nuclei and flat and loose cytoplasm; this layer is at the top of the epithelium.

Image analysis

Image analysis for the interim study was performed using an in-house modified version of the cyto-savant automated quantitative system (designed by our same research team and licensed by Oncometrics Imaging Corp., Vancouver, BC). This system includes a 12-bit, double-correlated sampling MicroImager 1400 digital camera (pixels, 6.8 m^2). This software was specially designed for the semi-automatic analysis of tissue sections. Thionine–Feulgen-stained nuclei were measured with a monochromatic light at a wavelength of 600 nm, using a ×20 0.75 numerical aperture plan Apo objective lens. With a printout of the diagnostic area in hand, a cytotechnologist located the same area on the Feulgen-stained slide as on the H&E-stained slide. As illustrated in Fig. 1, the cytotechnologist outlined with a mouse the basal membrane and the superficial membrane (Fig. 1A). These two membranes define the region of interest (ROI), or sampling window. Automatic detection of the nuclei (Fig. 1B) was then performed for further texture and architectural analyses. This procedure was fully automated and required only some minor manual changes. At a high magnification (×20), nuclear segmentation was performed within the ROI (Fig. 1C). Briefly, a thresholding algorithm was used to separate the objects (nuclei) from the background, based on pixel intensity [5]. The nuclear segmentation was manually corrected for adjacent objects. Finally, autofocusing and edge-relocation algorithms were applied to the nuclei to precisely and automatically place the edge of the object at the region of highest local gray-level gradient [4]. The digital gray-level images of these nuclei were stored in a gallery (Fig. 1D).

Quality control

The cytotechnologist manually reviewed each object in an image gallery of all the selected cells (Fig. 1D) and removed any object that did not fulfill the minimum requirements (e.g., bad mask, poor focus, pale nucleus, or pyknotic nucleus). Special attention is given to the lymphocytes to obtain a homogeneous population: only dark, dense, round objects are accepted. A quality assurance system guided the systematic collection of samples at both campuses [9,10].

Feature calculation

Nuclear features are extracted from the digitized nuclear images of each selected cell. Table 1 lists the features organized into different categories; approximately 120 features are calculated [4]. Morphologic features describe the nuclear size, shape, and boundary irregularities. The eight photometric features estimate the absolute intensity, optical density levels of the nucleus, and the intensity distribution.

Texture features

Discrete texture features were based on a threshold segmentation of the object into regions of low, medium, and high optical density. The thresholds are scaled to the sample staining intensity, as represented by the IOD norm value determined from the reference population. Details of algorithms for determining nuclear texture are described elsewhere [4]. Discrete texture features are by definition dependent on normalization. Markovian texture features characterize gray level correlation between adjacent pixels in the image. Non-Markovian texture features describe the local maxima and minima of gray-level differences in the object. Fractal texture features describe the local differences integrated over the object at multiple resolutions. Run-length texture features describe chromatin distribution in terms of the length of consecutive pixels with the same compressed gray level value along different orientations (0°, 45°, 90°, or 135°). To make the run-length features rotationally invariant, only the mean and standard deviation over the four directions were used for each run-length feature.

Statistical analyses

Definition of an HPV-associated change score

We defined HPV-associated changes (HACs) as changes induced by HPV infection in normal-appearing epithelial cells [6]. On the basis of our hypothesis that high-risk viruses induce more changes in the chromatin configuration, we generated an individual cell score, which was a phenotypic measure of the degree and intensity of deviation of an epithelial cell originating from an HPV-infected epithelium from a cell originating from healthy HPV-negative epithelium.

At the two extremes of this cellular scale, we first defined a group of cells selected from cervical specimens from the HPV–DNA-negative group of women and a group of cells from cervical specimens from HPV-16- and 18-positive women. A stepwise linear discriminant function analysis of data from these two groups generated a canonical score, or HAC score, which could then be calculated for any individual cell.

The cells were then randomly assigned to a training and validation set. The training set was classified using the HAC score. The validation set was similarly analyzed. The training and validation sets were compared. Analyses were then performed on per biopsy basis and finally on a per patient basis; i.e., in the former case any positive biopsy counted as a positive test and in the latter case, if any one biopsy was positive in a patient then the patient was considered HPV positive. All statistical analyses were performed with the Statistica software package (StatSoft, Inc., Tulsa, OK).

HPV testing

Cervical samples were tested for HPV using polymerase chain reaction (PCR).

Cervical cytobrush specimens were placed in micro-centrifuge tubes containing PBS with 0.05% sodium azide

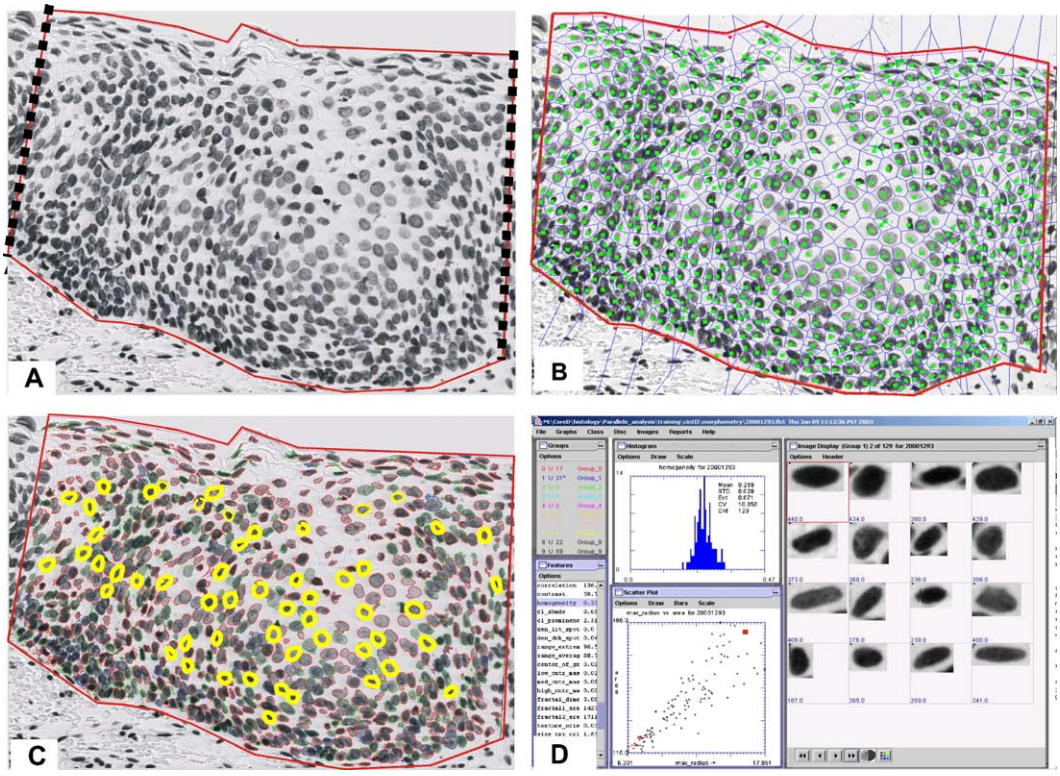

Fig. 1. Steps of the semiautomated analysis of cervical lesions: (A) definition of the ROI; (B) automatic locations of the positions of the nuclei; (C) automatic segmentation of the nuclei in the intermediate layers of the epithelium; (D) snapshot of the interface of our software used for postanalysis of the morphometric analyses (quality control).

and frozen at −20°. DNA was extracted using the QIAamp DNA Mini Kit (QIAGEN, Valencia, CA) after thawing. Brushes stayed in the tubes through the cell lysis step. The final volume of DNA was 110 μl. PCR was first performed with primers designed to amplify the glycerol-3-phosphate dehydrogenase gene (G3PDH), the housekeeping gene, to

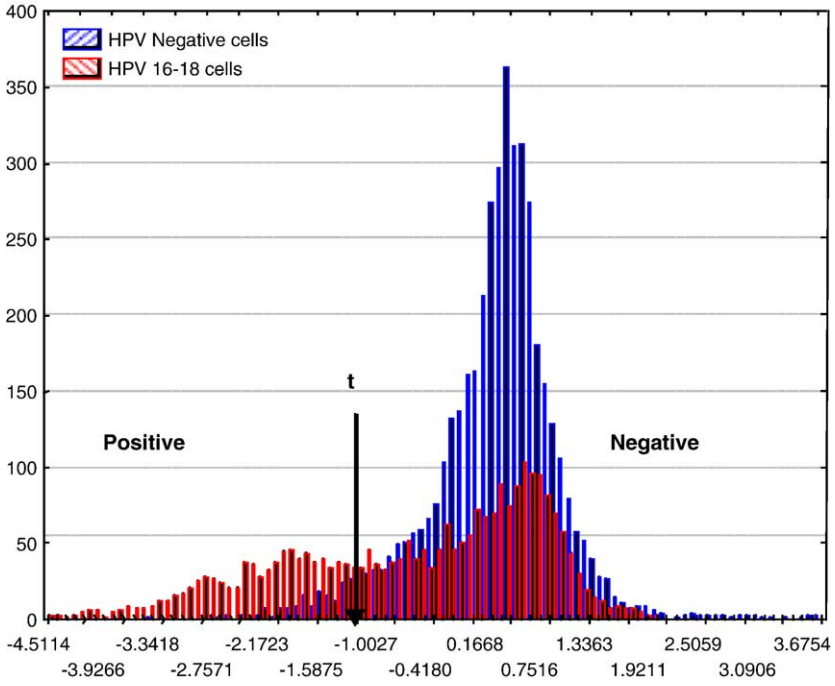

Fig. 2. Plot of morphometric score as a function of histopathology interpretation, generated from a linear discriminant analysis using 6 texture features: Range_extreme, LowAvgDistance, LowVsMedDNA, LowDNACompactness, GraylevelMax, and MediumCentreMass. HPV-positive cells are in red, and the HPV-negative cells are in blue. Placing a threshold at $t = -1$ allows a very favorable discrimination.

Table 1
Categories and features

Category	Features
	Cytometric features
Discrete texture [20]	Low, medium, and high DNA amount Low, medium, and high DNA area Low, medium, high, and medium_high DNA compactness Low, medium, high, and medium_high DNA average distance Low, medium, and high density object Low, medium, and high center mass Low_vs_medium, low_vs_high and Low_vs_medium-high DNA
Markovian texture [7]	Entropy, energy, contrast, correlation, homogeneity, cl_shade, and cl_prominence
Non-Markovian texture [5]	Density_light_spots, density_dark_spots, center_of_gravity, range_extreme, and range_average
Fractal texture [3]	Fractal_area1, fractal_area2, and fractal_dimension
Run length texture [20]	Short_runs_mean, short_run_stdv, short_run_min, and short_run_max Long_runs_mean, long_run_stdv, long_run_min, and long_run_max Gray_level_mean, gray_level_stdv, gray_level_min, and gray_level_max Run_length_mean, run_length_stdv, run_length_min, and run_length_max Run_percent_mean, run_percent_stdv, run_percent_min, and run_percent_max

ensure the integrity of the DNA. PCR products were resolved by electrophoresis in a 1.5% agarose gel and stained with ethidium bromide. Successful amplification was indicated by the detection of a 213-base pair product. Following the methods of Manos et al. [14], the samples were then analyzed for HPV–DNA using MY9 and MY11, consensus HPV primers that amplify a 450-base pair region of the L1 open reading frame of at least 28 different HPV types. The PCR products were then resolved by agarose gel electrophoresis, transferred to nylon membranes (Bio-Rad Laboratories, Hercules, CA), and hybridized to ^{32}P-labeled consensus HPV probe, an HPV-16-specific probe, and an HPV-18-specific probe, each on an individual membrane. DNA extracted from HPV-18-positive HeLa cells, HPV-16-positive Caski cells, and a negative control without DNA were used as controls in the PCR and subsequent hybridizations. The membranes were then analyzed by autoradiography.

Results

Patient samples studied

A total of 3275 biopsy specimens and 1544 Pap smears were clinically read for this study in 1544 patients. A total of 1420 quantitatively stained sections were analyzed with the imaging system. Inter- and intra-agreement studies of the data collected by all four devices at both institutions showed excellent agreement [9,10].

Those specimens found to be cytologically and histopathologically normal were chosen. There were 446 cervical biopsies selected from 248 women (mean age, 45.6 years; range, 18–80 years) enrolled in the diagnostic and screening studies. Using a classic cytologic interpretation method (3 independent reviews), study pathologists read the 248 smears 3 times and determined whether they were normal or within normal limits. They also read the biopsy specimens 3 times and determined whether they were normal or within normal limits. All specimens were squamous epithelium.

Patients were initially classified into 5 groups according the results of the PCR HPV–DNA test: HPV negative, HPV consensus positive, HPV 16 positive, HPV 18 positive, and HPV 16 and 18 positive (Table 2). Hybrid Capture results are also reported. Many of the samples came from the screening study and thus were HPV negative by PCR and HCII. Overall in this sample, 56% of patients were HPV positive by PCR and approximately 36% were positive by HCII. When the diagnostic study sample is separated from the screening study; that is patients with abnormal smears are considered alone, approximately 80% are positive by PCR and 60% by HCII in the larger sample of 1544.

Computation of the HPV-associated texture score

We define the HPV-associated changes (HAC) as changes in chromatin in normal-appearing epithelial cells. Under the hypothesis that high-risk viruses induced more changes in the chromatin configuration, we generated an individual cell score. This score was a phenotypic measure of the degree and intensity of deviation of the nuclear texture in an epithelial cell originating from an HPV-infected epithelium.

Of the 446 biopsies, 6977 cells were identified. On the two extremes of this cellular scale, we first defined a group of 4362 cells selected from cervical specimens from the HPV–DNA-negative group of women and then a group of 2615 cells from cervical specimens from HPV-16- and 18-positive women. Fig. 2 shows the distribution of the HPV canonical analysis. The t value is a composite of 6 selected features that were statistically significant in the linear discriminant analysis. They are as follows: Range_extreme,

Table 2
Sample size for the different groups

Group	HPV–DNA	Biopsy number	No. of patients	Age (range)
1	Negative	81	48	4 (31–64)
2	Consensus	180	101	43 (18–71)
3	HPV 16	89	46	44 (25–70)
4	HPV 18	49	25	49 (26–80)
5	HPV 16, 18	47	28	46 (26–60)
Total		446	248	

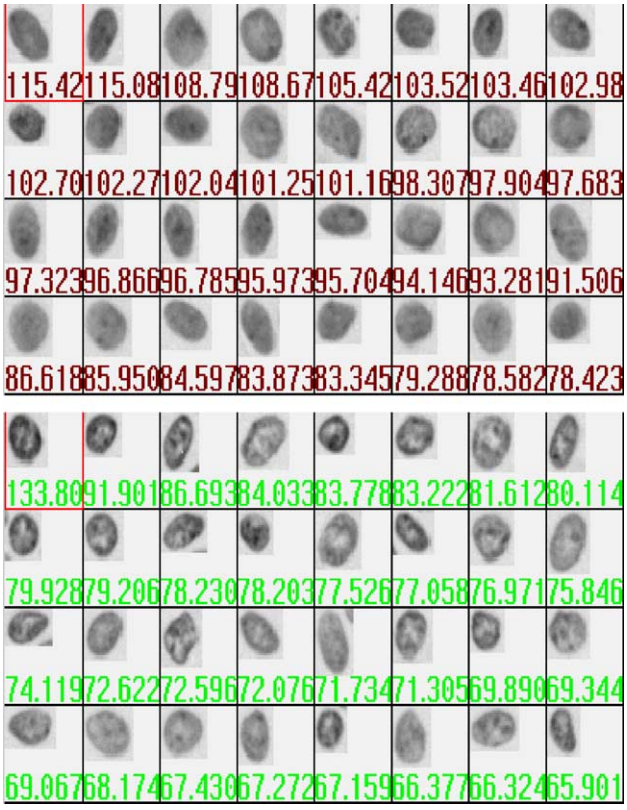

Fig. 3. Nuclear images of a subset of HPV-negative (top) and HPV-positive (bottom) cells from the current histopathologically negative sample.

LowAvgDistance, LowVsMedDNA, LowDNACompactness, GreylevelMax, and MediumCentreMass [4]. The t value is plotted on the abscissa while cell number is plotted on the ordinate. In this figure HPV-positive cells are in red, while HPV-negative cells are in blue. Placing a threshold at $t = -1$ allows a very favorable discrimination among the cell populations.

Use of the texture score to classify cells

Images of some typical cells classified as negative and positive are shown in Fig. 3. Nuclei from cells classified as HAC-positive have a more irregular chromatic organization – that is, more texture – than the HPV-negative cells. This can be seen by observing the two cell galleries. In the HPV-positive cell gallery, there are more dark areas in the nucleus compared to the fairly regular texture of the HPV-negative cells. These dark areas represent uneven areas of chromatin in the HPV-positive cells. The HPV-negative cells have even chromatin in the nuclei.

Table 3A
This analysis correctly classified 1723 of 2214 (78%) of HPV-negative cells and 687 of 1313 (52%) of HPV-positive cells in the training set

Predicted classification in training set				
Groups	Negative	HPV 16,18	Total	Correct classification (%)
Negative	1723	491	2214	77.8
HPV 16,18	626	687	1313	52.3
Total	2349	1178	3527	68.3

This classification matrix used a forward stepwise discriminant analysis to distinguish between the set of cells from biopsies from HPV-negative patients and the groups of cells from biopsies from HPV-16- and 18-positive patients. This yields a sensitivity of 52% and a specificity of 78%.

Table 3B
This analysis correctly classified 1645 of 2148 (77%) of HPV-negative cells and 707 of 1302 (54%) of HPV-positive cells in the validation set

Predicted classification in validation set				
Groups	Negative	HPV 16,18	Total	Correct classification (%)
Negative	1645	503	2148	76.5
HPV 16,18	595	707	1302	54.3
Total	2240	1210	3450	68.2

This classification matrix used a forward stepwise discriminant analysis to distinguish between the set of cells from biopsies from HPV-negative patients and the groups of cells from biopsies from HPV-16- and 18-positive patients. This yields a sensitivity of 55% and a specificity of 77%.

Results of training and test sets

The results of the discriminant analysis are given in Tables 3A and 3B. On the training set, Table 3A, this function correctly classified 1723 (78%) of the 2214 negative cells and 687 (52%) of the 1313 HPV-16- and 18-positive cells. In Table 3B, on the validation set, this function correctly classified 1645 of 2148 (77%) of HPV-positive cells and 707 of 1302 (54%) of HPV-negative cells. This function thus has a specificity of 77–78% and a sensitivity of 52–54% for this sample. The percentage of correctly classified cells was similar between the training and validation sets. This similar finding assures us of the randomness of the two samples, the even application of the function, and the validity of the findings.

Results applied to patient samples

In a study such as this one, in which multiple samples from each patient are obtained, two types of analysis can be performed. One can analyze the number of biopsies as though they were randomly distributed and one can analyze the patients such that any positive biopsy makes a patient positive; site by site or patient.

Table 4A
Frequencies of HPV-positive biopsies in the different HPV–DNA test groups

	HPV–DNA test by PCR by biopsy site					
	Negative	Consensus	16	18	16,18	Total
Negative	58	114	50	17	14	253
Positive	24	66	39	32	34	195
% Positive	33	38	49	66	70	43

Observed vs. expected frequencies: chi-square = 22.31754; $df = 4$; $P < 0.000173$.

Table 4B
Frequencies of HPV-positive patients in the different HPV–DNA test groups

	HPV–DNA test by PCR by patient					
	Negative	Consensus	16	18	16,18	Total
Negative	27	48	18	5	7	105
Positive	21	51	26	20	19	137
% Positive	43	51	59	80	73	56

Observed vs. expected frequencies: chi-square = 32.26826; $df = 4$; $P < 0.000002$.

Because many specimens had no HAC-positive cells, we defined a biopsy specimen as being HAC positive if it contained at least one HAC-positive cell. Table 4A shows the former analysis, looking at the biopsies and the number of HAC-positive and -negative specimens in the different HPV–DNA groups. Not surprisingly, the percentage of HAC-positive biopsy specimens increased steadily from the negative group to the HPV 16 and 18 groups. In addition, the frequencies of positive biopsy specimens in the different groups were statistically different from the expected frequencies based on the overall percentage of HPV-positive biopsies—43% (chi-square test: $P = 0.00017$) (Fig. 4).

A patient was considered HAC positive if at least one of her biopsy specimens was HAC positive. Table 4B shows the number of HAC-positive and -negative patients in the different HPV–DNA groups. Again, not surprisingly, the percentage of HPV-positive patients increased steadily from the negative group to the HPV 18 and the HPV 16 and 18 groups. In addition, the frequencies of HAC-positive patients in the different groups were statistically different from the expected frequencies based on the overall number of HPV-positive patients—56% (chi-square test: $P = 0.000002$).

Discussion

Our findings suggest correlations between HPV and chromatin condensation. We do not know the state of integration of HPV, and thus we cannot distinguish whether the specimens have abnormal texture due to HPV integration or chromosomal aneuploidy. Future studies will examine the integration of HPV by measuring E2 and E6/E7 expression.

Of further importance, these subvisual changes are observed and measured in cells from histologically normal-appearing epithelium from women with no histologic or cytologic abnormalities. While these preliminary results are interesting, the study needs to be repeated in a larger sample size, repeated on cytologic samples, and correlated with mRNA HPV levels. This is intended as more patients are accrued.

Texture features measure the degree of condensation and configuration of the chromatin and could be reflecting the phenotypic manifestations of HPV integration into the genome. This study is not designed to examine HPV integration. These concepts are somewhat established for precancerous lesions of the cervix [11–15]. Further biologic analyses will be performed to establish integration of HPV. Our approach was based on the development of an HPV phenotypic score that reflected the differences between cells from biopsy specimens from women with negative DNA–HPV test results and cells from biopsy specimens from women with positive DNA test results for HPV 16 and 18. The PCR test was used and arguably it is more sensitive than the HC II. The HC II has been FDA approved and the level of DNA measured is thought to be clinically relevant to the presence of disease. As we are studying the false negative and false positives of our gold standard, using PCR

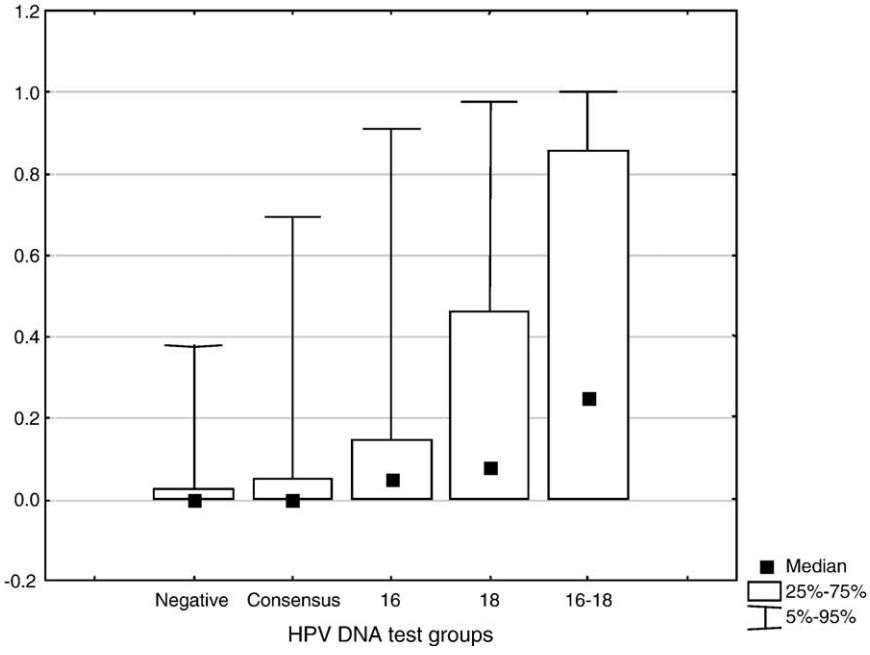

Fig. 4. Median frequencies of HPV-positive cells in negative biopsies per HPV diagnostic category using box and whisker plots.

was of interest. The statistical approach taken is similar to the approach taken to develop a classifier of cells from high-grade lesions used in quantitative cytologic diagnosis. The software used for the analysis has been validated with analyses in many organ sites [21].

Virtually all cervical cancers are HPV positive; HPV 16 and 18 are among the 5 types accounting for 80% of cervical cancers [1]. It was logical that these epithelial cells would show the most pronounced changes in chromatin and thus provide the best training set [16–18]. The integration of low-risk HPV types is different that high-risk HPV types. For example, HPV 18 is thought to integrate into cells more readily that HPV 16 (~100% with HPV 18 compared with ~75% with HPV 16). The data are similar in patients with head and neck cancer, in whom it has been shown that the viral integration in the host genome occurred in 46% with HPV 16 and in 20% with HPV 6 [19]. Finally, it seems that there are some differences between HPV 16 and HPV 18 in the degree and size of the region of integrated viral DNA produced by both viruses [20].

Future investigations will determine the real potential value of texture image analysis as an independent and quantitative test for HPV infection in cervical preneoplastic lesions of the cervix. Any single test integrating the measurement of the degree of dysplastic transformation and HPV infection is likely to become a diagnostic and prognostic tool for cervical cytologic and histopathologic examination. If the sensitivity and specificity of these analyses can be improved and if the findings are similar or better in cytologic samples, texture analysis may be a useful and cost-effective approach.

Acknowledgments

This research was supported by the National Cancer Institute under Program Project Grant 3PO1-CA82710-04. The authors thank Deanna Haskins, Anita Cairo, Laura Dillon, Tatiana Boiko, Iouri Boiko, Maria Valdizan-Garcia, Maria Teresa Arbelaez, Nan Earle, Chris King, and Trey Kell for their contributions to this project.

References

[1] Bosch FX, Manos MM, Munoz N, Sherman M, Jansen AM, Peto J, et al. Prevalence of human papillomavirus in cervical cancer: a worldwide perspective. International biology study on cervical cancer (IBSCC) study group. J Natl Cancer Inst 1995;87(11): 796–802.

[2] Wright TC, Cox JT, Massad LS, Twiggs LB, Wilkinson EJ. ASCCP-Sponsored Consensus Conference. 2001 consensus guidelines for the management of women with cervical cytological abnormalities. JAMA 2002;287:2120–9.

[3] Wright TC, Schiffman M. Adding a test for human papillomavirus DNA to cervical cancer screening. N Engl J Med 2003; 348:489–90.

[4] Doudkine AM, Poulin N, Palcic B. Nuclear texture measurements in image cytometry. Pathologica 1995;87:286–99.

[5] MacAulay C, Palcic B. An edge relocation segmentation algorithm. Anal Quant Cytol Histol 1990;12(3):165–71.

[6] Korbelic J, Matisic JP, MacAulay C, Garner D, Palcic B. Discrimination of mildly dyskaryotic squamous cervical cells with or without koilocytosis using nuclear features measured by quantitative histology and automated quantitative cytology. 21st European Congress of Cytology. Sept 12–16, 1993. Vienna, Austria, .

[7] Manos M, Ting Y, Wright D, Lewis A, Broker T, Wolinsky S. Use of polymerase chain reaction amplification for detection of genital human papillomaviruses. Cancer Cells 1989;7:209–13.

[8] Palcic B. Nuclear texture: can it be used as a surrogate end-point biomarker? J Cell Biochem 1994;19:40–6 [Supplement].

[9] Guillaud M, Cox D, Adler-Storthz K, Malpica A, Staerkel G, Matisic J, et al. Quantitative histopathological analysis of cervical intraepithelial neoplasia sections: methodological issues. Cell Oncol 2004; 26:31–43.

[10] Chiu D, Guillaud M, Cox D, Follen M, MacAulay C. Quality assurance system using statistical process control: an implementation for image cytometry. Cell Oncol 2004:1–17.

[11] Hanselaar AG, Poulin N, Pahlplatz MM, Garner D, MacAulay C, Matisic J, et al. DNA-cytometry of progressive and regressive cervical intraepithelial neoplasia. Anal Cell Pathol 1998;16(1):11–27.

[12] Poulin N, Boiko I, MacAulay C, Boone C, Nishioka K, Hittelman W, et al. Nuclear morphometry as an intermediate endpoint biomarker in chemoprevention of cervical carcinoma using alpha-difluoromethylornithine. Cytometry 1999;38(5):214–23.

[13] Artacho-Perula E, Roldan-Villalobos R, Salas-Molina J, Vaamonde-Lemos R. Histomorphometry of normal and abnormal cervical samples. Anal Quant Cytol Histol 1993;15(4):290–7.

[14] Weyn B, Tjalma W, Van De Wouwer G, Van Daele A, Scheunders P, Jacob W, et al. Validation of nuclear texture, density, morphometry and tissue syntactic structure analysis as prognosticators of cervical carcinoma. Anal Quant Cytol Histol 2000;22(5):373–82.

[15] Keenan SJ, Diamond J, Glenn McCluggage W, Bharucha H, Thompson D, Bartels PH, et al. An automated machine vision system for the histological grading of cervical intraepithelial neoplasia (CIN). J Pathol 2000;192(3):351–62.

[16] Cullen AP, Reid R, Campion M, Lorincz AT. Analysis of the physical state of different papillomavirus DNAs in intraepithelial and invasive cervical neoplasm. J Virol 1991;65:606–12.

[17] Das BC, Sharma JK, Gopalakrishna V, Das DK, Singh V, Gissmann L, et al. A high frequency of human papillomavirus DNA sequences in cervical carcinoma of Indian women as revealed by Southern blot hybridization and polymerase chain reaction. J Med Virol 1992;36: 239–45.

[18] Berumen J, Casa L, Han S-H. Genome amplification of human papillomavirus types 16 and 18 in cervical carcinomas is related to the retention of the E1/E2 genes. Int J Cancer 1994;56:640–5.

[19] Venuti A, Manni V, Morello R, De Marco F, Marzetti F, Marcante M. Physical state and expression of human papillomavirus in laryngeal carcinoma and surrounding normal mucosa. J Med Virol 2000;60(4): 396–402.

[20] Corden SA, Sant-Cassia LJ, Easton AJ, Morris AG. The integration of HPV-18 DNA in cervical carcinoma. J Clin Pathol Mol Pathol 1999;52:275–82.

[21] Kamalov R, Guillaud M, Haskins D, Harrison A, Kemp R, Chiu D, et al. A Java application for tissue section image analysis. Comput Methods Programs Biomed 2005 (Feb);77(2):99–113.